Novel Stemless Hip Prosthesis Design and Finite Element Analysis to validate stemless Prosthesis for Reduction of Aseptic Loosening in Total Hip Arthroplasty

Nishan Khadka[1*], Mukesh Yadav[2*], Adhish Ghimire[3]

[1]Department of Mechanical and Aerospace Engineering, Pulchowk Campus, Institute of Engineering, Tribhuvan University, Lalitpur, Nepal.
[2]Department of Mechanical Engineering, Delhi Technological University, Delhi, India.
[3]Manipal Medical College, Kathmandu University, Pokhara, Nepal.
Corresponding: [1*]072bme626nishan@ioe.edu.np; [2*]mukeshyadav_bt2k16@dtu.ac.in

---

Abstract

Total Hip Arthroplasty/ Replacement is a major corrective procedure involving replacing the femoral head and neck of the long bone connected to the pelvis. Conventional methods involved long-stemmed Titanium Alloy (Ti_6Al_4V) implants with a Cobalt-Chrome (Co-Cr) spherical caps. The invasiveness, large distributions of interfacial stresses induce stress shielding and bone resorption leading to loosening and painful remission surgeries, specifically in the younger, more active individuals. The need to improve upon the less invasive stemless models is warranted. This paper incorporates an improved novel design to a stemless hip prosthesis. Finite element analysis concluded average stresses of 9MPa, average strains of 0.0063 mm/mm, total deformation of 88mm all within close ranges and better than conventional long-stemmed models as a prosthesis for an exaggerated point load of thrice the body-weight of a human (867N) taken redundantly. Fatigue life is better than traditional models crossing 10^{10} cycles for extreme loading. The contact stresses also proved to be lesser and spread over a smaller area reducing the chances of aseptic loosening compared to conventional models.

Keywords: Total Hip Arthroplasty, Hip prosthesis, Long-Stem implants, Stem-less implants, Finite Element Analysis, Aseptic Loosening, Stress Distribution

1.0 Introduction

The Hip joint connects to one of the largest weights bearing members of the human body. Naturally, the hip joint is a ball-socket joint responsible for a wide range of motion and physical activities and weight-bearing functionality of the immediate area and parts of the neck, head, upper body, making it crucial in several static and athletic activities [1,2]. The Hip joint consists of a cup-shaped acetabulum supplied by a layer of lubricating synovial fluid. The acetabulum is the pelvis part which forms the “Socket” of the Hip joint. The femur’s head is roughly spherical and sits comfortably in the Acetabulum, forming a Ball and socket joint. The head of the femur is attached to the femoral neck, which is inclined (150° for child <150° for adults) with respect to the femoral shaft (central lining of the femur) [1] which connects to the lower body. The assembly is supported by an assortment of ligaments [2].

The Hip joint is subjected to wear and tear and even breakdown in the case of certain diseases like rheumatoid arthritis, osteoarthritis, fractures, and dislocations or fracture due to accidents [3]. The

wear and tear of the Hip joint is also typical with aging. Based on the severity of the condition and the patient's biological information, Total Hip Replacement of Total Hip Arthroplasty could be recommended. THA or THR is the total replacement of the Ball and socket joint of the Hip with prosthetics materials like metal or plastic to rectify the problems associated with diseased or corrupted Hip joints [2]. THA is a prevalent procedure that aims to restore mobility with over 500,000 surgeries per annum projected in the US alone by 2030 [5]. Worldwide, the THA procedure occurs in millions [4].

THA is a very intricate process that involves managing forces on the hip joint extensively to account for different motion ranges such as jogging, walking, running, jumping, and so forth [6]. Typically, THA involves one of three methods based on the severity and patient's age. They are cemented methods (using cement of compounds like Methyl Methacrylate), Hybrid methods and Non-cemented methods [27]. The popular method is to have an implant impinge into the femoral shaft or femoral cavity [6]. Pioneered by Charnley in the 1960s, this method is quite common with THA's contemporary design and development. While the premise is entirely warranted for a successful THA, an invasive prosthesis elicits preventable problems in the future [28].

The problem with invasive prosthesis or the traditionally long-stemmed implants leads to excessive stress shielding and thigh pain [8]. It has been observed that most of the implant's failure is caused by the aseptic loosening of the implants [11]. One of the reasons of aseptic loosening is "Osteolysis", which is the process of progressive destruction or disappearance of bone tissue [9], consequently leading towards the implant's failure. Microparticles are released from the femoral head when connected to the acetabular cup, leading to the progressive wear of the implant, causing osteolysis and resulting in aseptic loosening [8]. 10% of THR have Revision surgery within 10 years, bad design leads to complications and the average life-span tends to be 15 years. Revision surgery may lead to inoperable fractures [12]. It has been observed that the revision surgery is more substantially more complicated than the initial surgery as it is required to remove the previous implant, making it much complicated than it would have been normally [9]. After the completion of surgery, the patients are more susceptible to complications, causing the recovery to take a longer time making it a riskier process, costly and inconvenient for the patients [10,11]. Thus, efforts are made to make prosthetics life longer. Long-stemmed prosthesis is a satisfactory procedure for the elderly; however, aseptic loosening and fracture make it highly inconvenient for the youth (<60) [33].

The typical design of THA prosthesis in contemporary medicine consists of a "of a femoral stem, a femoral head (ball) that attaches to the stem, an acetabular cup and a fixation agent to secure the stem into the femur and the acetabular cup into the acetabulum in the pelvis" [7]. To qualify the implant's invasiveness and reduce remission surgeries, different stemless and short-stemmed designs have emerged since early development of the Hip prostheses [27]. Short-stemmed design has been excellent to improve load transfer and circumvent some of the problems incurred by invasive long-stemmed implants making it suitable for youth [14,15,16]. Munting and Verphelen [13] introduced a short rod implant with several bolts for fixation. This step towards entertaining the problem of invasiveness was positive but curtailed by the use of metal bolts on brittle bones. The stemless design addressed the biocompatibility question by Suresh G. Advani et al [14], where

belts were used for fixation, to the less invasive bolts. This paper intends to improve upon the previous designs of the stemless hip prosthesis while being objective about the reduction of stress shielding and aseptic loosening.

2.0 Methodology

2.1 Design

The hip prosthesis was based on previous stemless designs by Advani S, [14] and Munting and Verphelen [13]. The CAD models were created on SolidWorks 2018. The femur's CAD file was derived from Grab CAD [18], which incorporated a CAM based on CT scanned imaging of an actual femur [15]. The models included: - (a) the unfeigned CAD model of the femur as a control group, (b) the popular Ti6AI4v prosthesis [19] for comparison, and (c) the proposed model by this paper.

SolidWorks 2018 was used as the primary CAD software to model the prosthesis. The contemporary design of the prosthesis consists of an acetabular cup made from Cobalt-Chrome (Co-Cr), which fits into the acetabular cavity (acetabulum) of the pelvic bone of the average human being [1]. The rest of the prosthesis consists of a Titanium Alloy (Ti6Al4V) stemmed implant, which is the modification of Charnely's original prosthesis [19]. The acetabular cup is a sphere of 16mm radius, which leads to a femoral neck (implant neck) of 12 mm, which is 15mm at thickest, 15mm in length, which is connected to a stem banked at 135° [1]. The stem is 16mm at its thickest (proximal end) and 12mm at the distal end [19,24]. The 3D model is represented in fig 1.

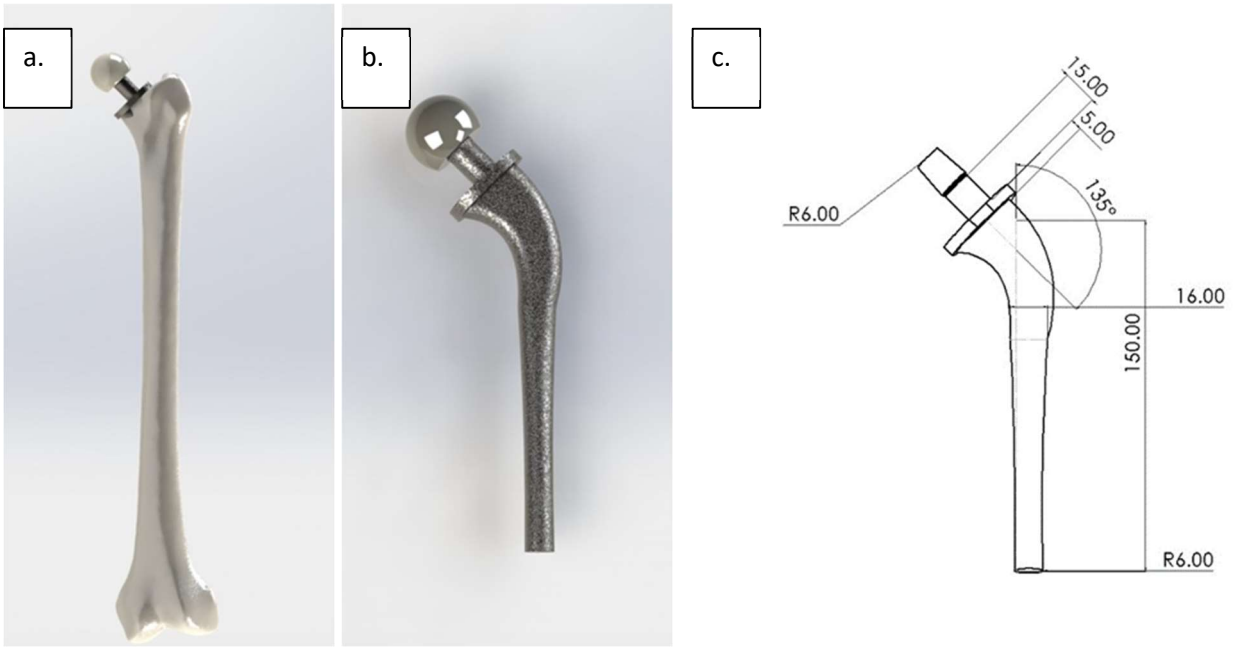

.

Figure 1 **a)** 3D model of the conventional prosthesis implanted into the femoral cavity **b)** 3D model rendering of the conventional prosthesis [19,24] consisting of the acetabular head **c)** 2D drawing of the CAD model of the prosthesis highlighting salient dimensions in mm.

This paper's new and proposed design entails changes made to the original Munting and Verphelen [13] and the Advani S, [14]. The implant comprises an acetabular cap (16mm spheroid), which is to be placed in the pelvis's acetabulum. It leads to a short neck of 15mm in length and 10mm in diameter. The neck connects to the flat plate that is common with the stemmed prosthesis but is broader. The plate's distal part is fitted with two M2 studs placed 10 mm apart and protruding through the femur. The studs are fitted with internal screws. On the space between the Quadratus femoris and the iliopsoas muscle, a small 15mm cavity is made on the femur where the distal plate is fitted. The plate also consists of M2 holes for two M2 Polyurethane ANSI metric 18.36 countersunk screws placed 10mm apart and inclined with the upper plate's distal end. This way, using the screw and minimal invasion of the femur, the implant is secured onto the femur.

Further, use of Stainless-steel wires is attached to the two plates to provide extra protection against failure. The implant body is made up of the conventional Ti6Al4V alloy. The acetabulum is made up of ceramic, which fits over the implant's neck. The use of lateral screws is intended to remove the invasiveness with Muting [13], and the SS wires are intended to reduce loosening prevalent in Advani S [14]. Further, the use of polyurethane sockets and screws are assumed to eliminate bio-compatibility issues with affixation as metal screws are inherently tricky to fit inside the brittle bone material [34]. The illustrations are represented in fig 2.

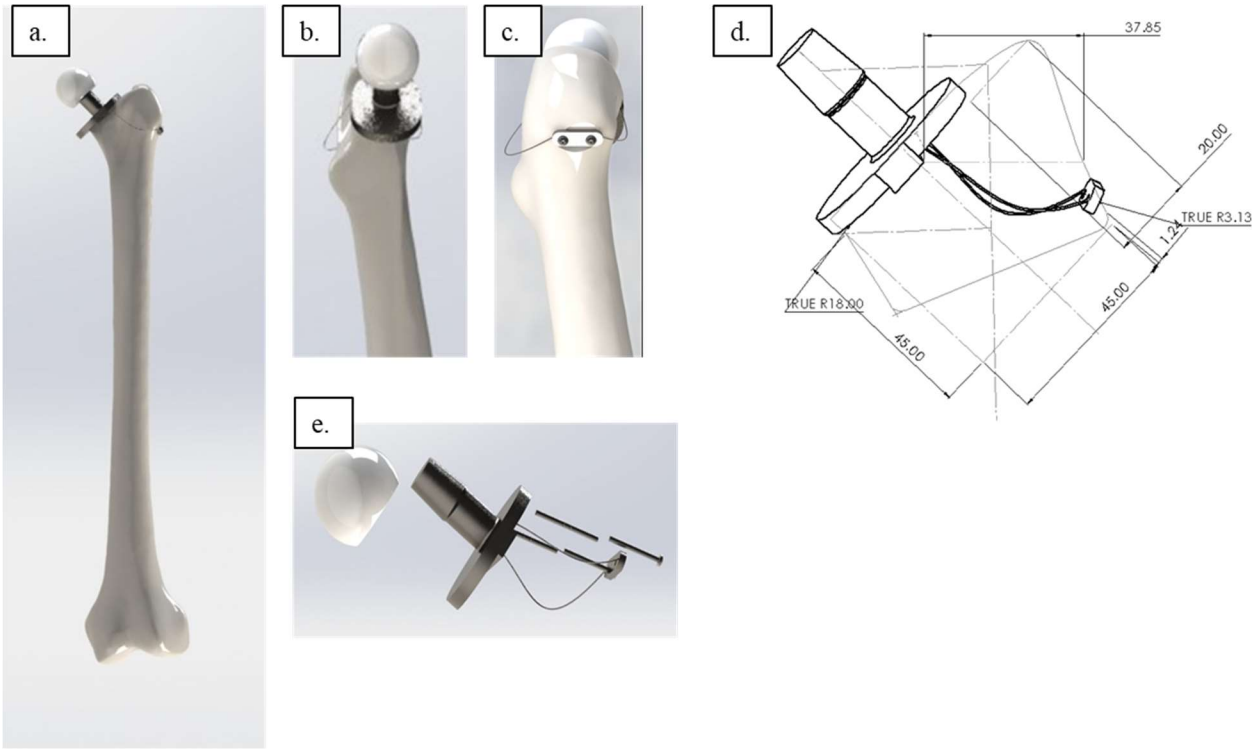

Figure 2 **a)** 3D model rendering of the proposed no-stem prosthesis design affixed onto the femur **b)** Back View of the proposed no-stem prosthesis design with the femur **c)** Front View of the proposed no-stem prosthesis design with the femur **d)** 2D drawing of the implant model with dimensions in mm. **e)** 3D model rendering of the proposed no-stem implant with acetabular head.

2.2 Numerical methods

The finite element analysis of the three groups under study was carried out using ANSYS 2019. The control group was taken as a normal femoral bone [15], while study group 1 included a conventional prosthesis model based on modified Charnely's stemmed prosthesis, as shown in figure 1. The proposed model or study group 2 comprised of the no stem model fixed onto the femur. The primary study area included static analysis viz. deformation under the loading conditions, Von-Misses Stresses, Total Elastic Strain, and fatigue under cycling loading conditions. The study aimed to determine the proposed model's integrity with a conventional counterpart within the extreme limits of loading conditions.

2.2.1 Materials and Method

Isotropic properties were considered in the FEA of the study groups. For the FEA, each material requires properties regarding their Young's Modulus of Elasticity (GPa) and Poisson's ratio. Further, analysis of fatigue life requires Yield Strength and the tentative Stress-Total Life to failure (S-N) curve data. The relevant data is tabulated in Table 1

The human bone comprises a mineral composition with organic and inorganic materials like hydroxyapatite and water. Based on several factors, bones can be classified into cortical bones, ligaments, cancellous bone, cartilage. Median values were taken off the Isotropic properties [25].

For the implant, the acetabular head was comprised of Cobalt-Chrome, while the implant body for both the stemmed implant and stemless implant was made up of Titanium alloy (Ti6Al4V). For the stemless implant, the fixation method involved the use of glass-reinforced polyurethane screws [35,36] and thin strips of structural stainless steel.

The properties of the material are shown below:

Table 1 Materials used in the 3D model's FEA along with its isotropic properties of Young's modulus of elasticity Poisson's Ratio, and Compressive Yield Strength

Components	Materials	Elastic Modulus (GPa)	Yield Strength (GPa)	Poisson's Ratio
Femoral Stem and Metal Shell	Titanium Alloy Ti_6Al_4V	110	0.88	0.32
Femoral head Inner liner (acetabular cap)	Cobalt-Chrome (Co-Cr)	220	0.76	0.31
Bone	Collagen+ calcium phosphate	10	0.15	0.15
Harness	Stainless Steel	200	0.25	0.3
Screws	Glass-fiber reinforced Polyurethane	72.3	1.95	0.2

2.2.2 Loading Conditions

The femur head and the neck are assumed to be rigid bodies to improve computational efficiency. The average human of 1.7m in height weighs about 75 kg. For redundancy, this data is taken as 867N in terms of weight. In a one-legged stance, the human hip naturally can support three times its weight without any aggressive damage to the hip joint [20]. Therefore, a load equivalent to 2500N was applied to the acetabular cap in either case in the X- horizontal and Y-vertical axis directions. A net equivalent force acts along the femoral neck axis in either the natural bone, stemmed, or stemless implant, i.e., 135° with the horizontal. Loads in the z-axis were avoided deliberately to only the calculation and maintain the implant and bone deformation in the 2D plane.

For supports, musculature was not considered to evade complications. Rigid support was applied at the distal end of the long bone, which signifies the beginning of the human anatomy's knee joint [1].

2.2.3 Setting up for FEM

The control group was affixed onto the XY plane with its central axis parallel to SpaceClaim's y-axis. For study group 1, i.e., a conventional stemmed model of the hip implant, Boolean operations were carried out in the design modular to create a cavity in the femur, and subsequently, the contact zones were defined. The acetabular cap was bonded with the implant's femoral neck, and the contact region of the stem of the implant and the femoral cavity was considered Rough in the Mechanical Modeler. The proposed stemless design was also similarly modeled in ANSYS. Boolean operations were carried out to remove the part of the femur for affixation. Contact between the implant's inner parts with the femur was considered Rough while the screws were bonded onto the femur.

Each study group consisted of meshing with default triangular elements of the mechanical modeler in ANSYS. For the implants, mesh density was increased at the plane of contact to avoid convergence errors in the ANSYS solver and obtain a degree of accuracy in the salient regions. The mesh quality details are tabulated in table 2, and the Mesh is shown in Fig 3.

Table 2 Statistics of Mesh in terms of number of nodes and elements in respective study group.

Model	Number of Nodes	Number of Elements
Conventional model in femur	61357	34834
Femur without implant (control)	31056	17630
Proposed stemless design	40442	21233

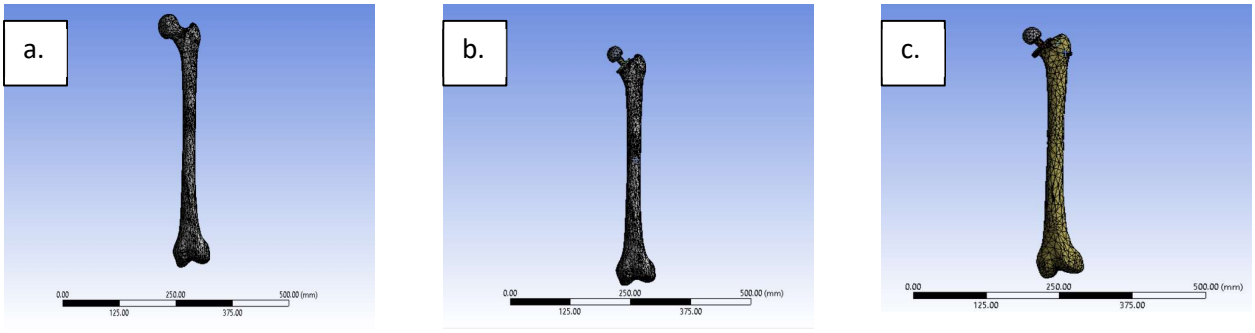

Figure 3 **a)** 3D model of the meshed femur (control) **b)** 3D model of the meshed conventional stem hip prosthesis **c)** 3D model of the meshed proposed stemless hip prosthesis

3.0 Results & Discussion

The static analysis of the hip joint was carried out for three different study groups a) femur bone (control group), b) conventional stemmed hip prosthesis implanted on the femur c) Proposed stemless hip prosthesis affixed on the femur. The FEA of each model is represented from figures 4 to 9.

3.1 Total Deformation

The prosthesis and the control group subjected to the boundary conditions as stated in 2.2.2 showed some amount of deformation, which is tabulated in Table 3, and the deformation plots are represented in fig 4.

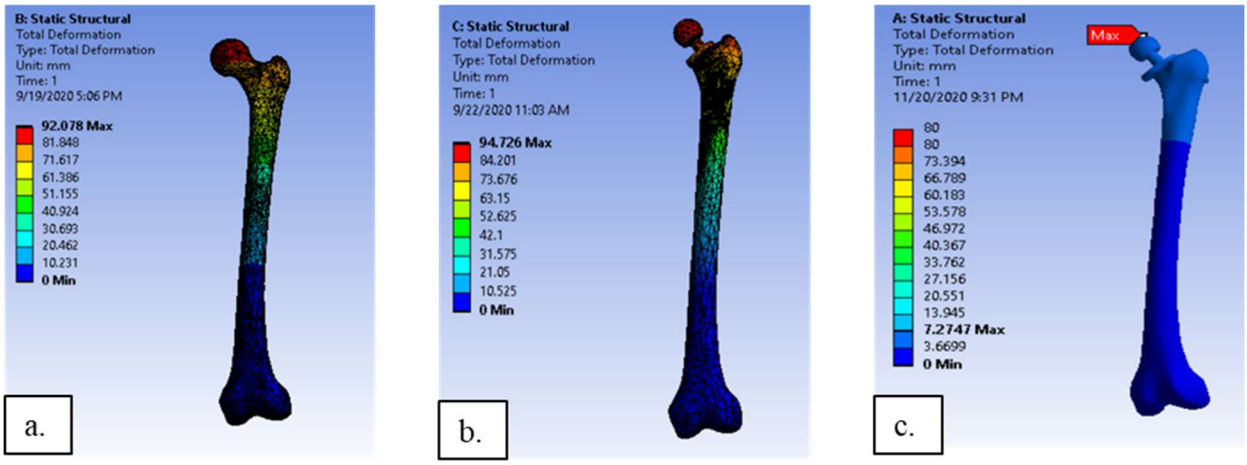

Figure 4 Total deformation plot of **a)** Natural Femur(control) **b)** Conventional stemmed hip prosthesis implanted onto the femur **c)** proposed stemless hip prosthesis affixed onto the femur.

It can be seen that the maximum deformation is seen in the femoral head of the bone, which is represented by the red region, which gradually decreases towards the bottom. The magnitude of the range of deflection is represented in table 3. The proposed stemless implant has a maximum

deflection of 7.247 mm, which is less compared to the conventional stemmed implant (94.736 mm) and the natural femoral bone (92.078 mm). Incidentally, deformation is also mainly nearing the top of the proximal part of the femur. This is also common to the uppermost part of the implant in the stem-less model. From the results of static analysis of the conventional stemmed implant, it can be seen that the maximum deformation is observed in the head region of the implant, similar to the results seen in the analysis of bone alone. Because of the concentrated load being applied at that point in the implant, which is not common pragmatically [29]. However, extreme data is warranted for the study.

Table 3 Range of displacement from Total Deformation plot in the respective study group

Model	Maximum displacement(mm)	Minimum displacement(mm)
Femur without implant (control)	92.078	0
Conventional model in femur	94.726	0
Proposed stemless design	7.274	0

Total or Equivalent Stresses

The maximum von-mises stress can be seen in the bone's shaft part in both the standalone femur(control) and the stemmed implant. However, the stemmed implant's neck shows appreciable stress in the order of nearly 42MPa, which is consequential of the short neck in the implant. Similarly, the neck in the proposed stemless design shows appreciable stress in a similar range, albeit lower than 40MPa. Stress is also well within limits in the plane plate of the proposed design. Stress concentrations exist in the stemless implant's fixation area, which increases its magnitude to a maximum of 344.73 MPa but is still lower than the maximum stress observed in the conventional model for the same boundary conditions. The stress distribution is represented in the Figure 4 where range of stress is represented by the colour contour in the figure.

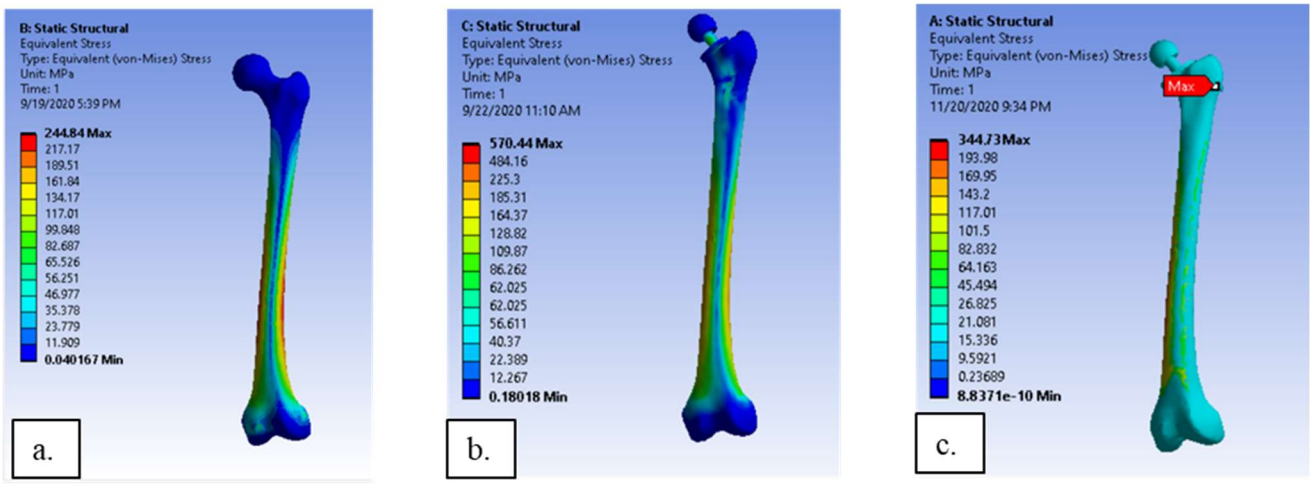

Figure 5 Total or Equivalent (von-Misses) Stress plot of **a)** Natural Femur(control) **b)** Conventional stemmed hip prosthesis implanted onto the femur **c)** proposed stemless hip prosthesis affixed onto the femur.

The static analysis of the proposed stemless implant shows similar results for the deformation as in the previous designs. The stress distribution, however, with the use of probes can be seen greater in the areas of fixation i.e. the polyurethane screws. This is due to the presence of localised stresses in a relatively small area of fixation [30].

Table 4 Range of displacement from Total Deformation plot in the respective study group

Model	Maximum stress (MPa)	Average Stress (MPa)	Minimum stress (MPa)
Femur without implant (control)	244.84	38.672	0.007292
Conventional model in femur	570.44	25.628	0.18018
Proposed stemless design	344.73	22.318	8.8×10^{-10}

In terms of average stresses, it can be inferred from table 4 in the standalone femur; it is less than the conventional model; however, the stress is even lower in the proposed design. This implies that the proposed design's stresses are not large enough to cause any appreciable damage compared to the conventional model. However, unbalanced stress distributions are possible due to the low average stress in the proposed model.

Interestingly from figure 5, it can be observed that the thin wire used as a harness to support the implant on to the femur absorbs some amount of stress in the order of a few MPa, which can be advantageous to preclude failure in the main body and movement standard in stemmed implants.

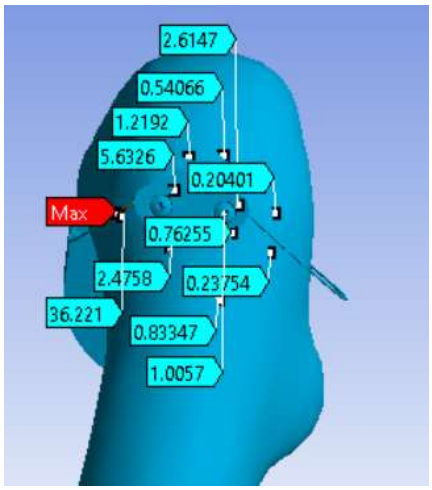

Figure 6 Back view of the proposed stemless implant head showing stress distributions using probes.

Equivalent Strain

The plot of the equivalent strain in each of the study group is represented in figure 6. The values of strain are tabulated in table 6.

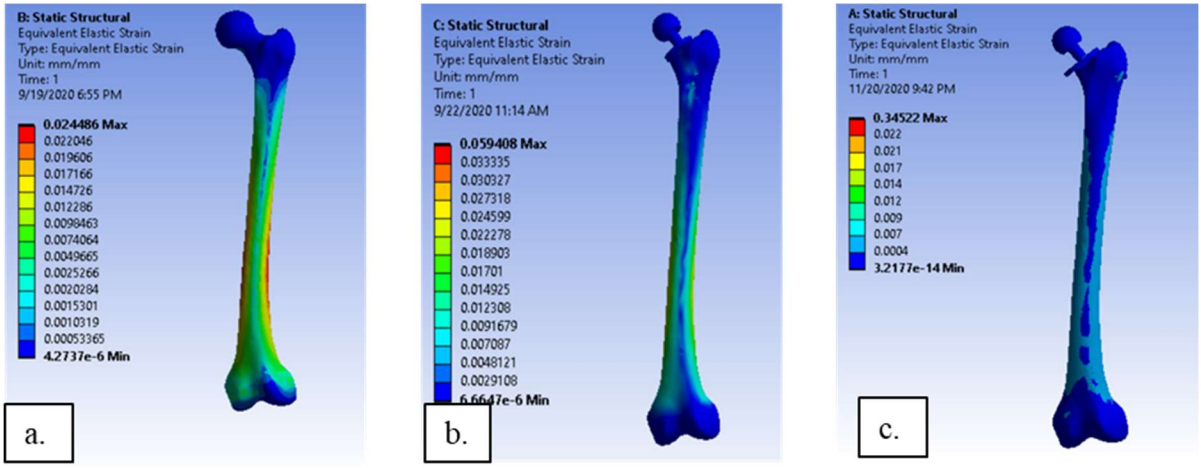

Figure 7 Total or Equivalent Elastic Strain plot of **a)** Natural Femur(control) **b)** Conventional stemmed hip prosthesis implanted onto the femur **c)** proposed stemless hip prosthesis affixed onto the femur.

The values of maximum strain in natural bone and the proposed prosthesis are comparable. However, maximum strain in the conventional design is high, which is expected because of the localized stresses discussed above [30]. Maximum straining occurs at the femoral shaft for each design. The low average strains in either of the prosthesis suggest a poor distribution similar to the stress range.

Table 5 Range of displacement from Total Deformation plot in the respective study group

Model	Maximum strain (mm/mm)	Average Strain(mm/mm)	Minimum strain (mm/mm)
Femur without implant (control)	0.0244	0.0038	4.2736×10^{-6}
Conventional model in femur	0.0594	0.00259	6.6647×10^{-6}
Proposed stemless design	0.34522	0.0003233	3.2117×10^{-14}

The average strain for the proposed stemless design is more significant than the least valued standalone femur and the comparable conventional model. The biggest drawback is the localized strain in the new model; however, the average values are within the limit [20].

Fatigue Life Analysis

Fatigue life analysis of the analysis was also conducted for the conventional stemmed implant, and the proposed stemless implant with load considered a reversed cyclic load. The Total life plot of each implant is presented in figure 7.

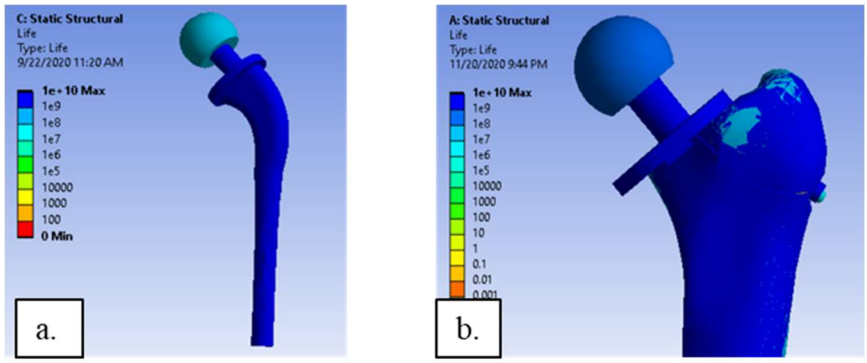

Figure 8 Fatigue life distribution plot of **a)** Conventional stemmed hip prosthesis **c)** proposed stemless hip prosthesis affixed onto the femur.

From the result, it was observed that the life of the stemless implant was very comparable to the conventional model in terms of fatigue failure. The issue with the conventional model was with a lower life for the Co-Cr head while the polyurethane screws has a slightly lower life in the proposed design.

Conclusions

The new stemless model for hip prosthesis was successfully created based on the older stemless designs' efficacy and shortcomings. The novel prosthesis was analyzed for stress distributions, deformation, strain, fatigue life, and interfacial stresses using FEA, and the results were compared with the FEA of standalone Femur as a control group and the conventional design of the long-stemmed hip prosthesis.

The FEA yielded reduced deformation compared to that of the other study group at around 7.27 mm for an excessive force of thrice the bodyweight of a human being (87kg). The results were followed by average stress distributions of approximately 9 MPa in a becoming range (~minimal-344MPa), which is a good value compared to the other study groups. This was also the case for strain distribution as both range, and average values were lower than the conventional and comparable to the natural bone. The fatigue life was much better with the new prosthesis as compared to the conventional model and the contact stresses induced minimal contact with proper stress distribution, which compared to the high valued, broad surface stress distribution of the conventional model was better at reducing stress shielding and subsequently bone resorption and aseptic loosening [32]. Further, the minimally invasiveness and ease of access during remission surgeries favor the proposed design.

The design alone would stand as a better, less invasive, more durable alternative. However, certain aspects could ameliorate stemless prosthesis. The issue of biocompatibility downplays any model as a substitute. The use of biocompatible material with a compact design will reduce localized stresses and prevent failure and improve internal body health. Also, better fixation methods will be conducive to perpetuating the stemless implant ideology as a staple form of prosthesis, especially for the active individual.

References

1. Byrne, Damien & Mulhall, Kevin & Baker, Joseph. (2010). *Anatomy & Biomechanics of the Hip.* The Open Sports Medicine Journal. 4. 10.2174/1874387001004010051.
2. Sivasankar, Murugaiyan &., s.Arunkumar & Velu, Bakkiyaraj & Muruganandam, A & Sathishkumar , S. (2016). A Review on Total Hip Replacement. 10.13140/RG.2.2.13686.80969.
3. Kurtz S, Ong K, Lau E, Mowat F, Halpern M. Projections ofprimary and revision hip and knee arthroplasty in the UnitedStates from 2005 to 2030. J Bone Joint Surg Am Volume2007;89(4):780e5.
4. Derar, H., & Shahinpoor, M. (2015). *Recent Patents and Designs on Hip Replacement Prostheses. The Open Biomedical Engineering Journal, 9(1), 92–102.* doi:10.2174/1874120701509010092.
5. Byrne, Damien & Mulhall, Kevin & Baker, Joseph. (2010). *Anatomy & Biomechanics of the Hip.* The Open Sports Medicine Journal. 4. 10.2174/1874387001004010051.
6. Sivasankar, Murugaiyan &., s.Arunkumar & Velu, Bakkiyaraj & Muruganandam, A & Sathishkumar , S. (2016). A Review on Total Hip Replacement. 10.13140/RG.2.2.13686.80969.
7. Clarke A, Pulikottil-Jacob R, Grove A, et al. Total hip replacement and surface replacement for the treatment of pain and disability resulting from end-stage arthritis of the hip (review of technology appraisal guidance 2 and 44): systematic review and economic evaluation. Southampton (UK): NIHR Journals Library; 2015 Jan. (Health Technology Assessment, No. 19.10.) Chapter 1, Background. Available from: https://www.ncbi.nlm.nih.gov/books/NBK273961/
8. L.A. Reynolds and E.M. Tansey, Eds*, Early development of total hip replacement*, Wellcome Witnesses to Twentieth Century Medicine, vol. 29. Wellcome Trust Centre for the History of Medicine at UCL: London 2007.
9. K.J. Saleh, I. Thongtrangan, and E.M. Schwarz, "Osteolysis: medical and surgical approaches", Clinical Orthopaedics and Related Research, no. 427, pp. 138-147, October 2004.
10. S. Srimongkol, "A review of mathematical modelling in total hip replacement", International Mathematical Forum, vol. 7, no. 52, pp. 2561-2569, 2012.
11. D. Snyder, R. Chapell, W. Bruening, K. Schoelles, J. Kaczmarek, E. Kuserk, and E. Erinoff, "Horizon Scan on Hip Replacement Surgery", ECRI Evidence-Based Practice Center, Rockville, MD, Rep. 290-02-0019, December 22, 2006.
12. Sargeant, and T. Goswami, Hip implants: Paper V. Physiological effects, Elsevier Materials and Design, vol. 27, pp. 287-307, 2006.
13. Kurtz S, Ong K, Lau E, Mowat F, Halpern M. Projections ofprimary and revision hip and knee arthroplasty in the UnitedStates from 2005 to 2030. J Bone Joint Surg Am Volume2007;89(4):780e5.
14. BergmannG, *et al*, 1993, Hip joint loading during walking and running, measured in two patients, Journal of Biomechanics, 26, 969-990.

15. Derar, H., & Shahinpoor, M. (2015). *Recent Patents and Designs on Hip Replacement Prostheses. The Open Biomedical Engineering Journal, 9(1), 92–102.* doi:10.2174/1874120701509010092
16. Logroscino, G., Donati, F., Campana, V., & Saracco, M. (2018). Stemless hip arthroplasty versus traditional implants: a comparative observational study at 30 months follow-up. HIP International, 28(2_suppl), 21–27. https://doi.org/10.1177/1120700018813209
17. E. Munting, M. Verhelpen(1995), Fixation and efect on bone strain pattern of a stemless hip prosthesis, J. Biomech. 288) 949–961.
18. S.G. Advani, M.H. Santare, F. Miller, and M. Joshi (2002), "Stemless hip prosthesis", U.S. Patent 6,379,390 B1.
19. Rawal, B R & Ribeiro, Rahul & Malhotra, Rajesh & Bhatnagar, N.. (2011). Design and Manufacture of Short stemless Femoral Hip Implant based on CT Images. Journal of Medical Sciences (Faisalabad). 11. 296-301. 10.3923/jms.2011.296.301.
20. Asgari, S. & Hamouda, A.M.S & Mansor, Shattri & Singh, Harwant & Mahdi, Elsadig & Wirza, Rahmita & Prakash, B.. (2004). Finite element modeling of a generic stemless hip implant design in comparison with conventional hip implants. Finite Elements in Analysis and Design - FINITE ELEM ANAL DESIGN. 40. 2027-2047. 10.1016/j.finel.2004.02.003.
21. Yan, Shuanggen & Chevalier, Yan & Liu, Fanxiao & Hua, Xingyi & Schreiner, Anna & Jansson, Volkmar & Schmidutz, Florian. (2020). Short Stem Hip Arthroplasty Provides a More Physiological Load Transfer: a Comparative Finite Element Analysis Study. 10.21203/rs.3.rs-53386/v1.
22. Isaza, Enrique & García, L & Salazar, E. (2013). Determination of Mechanic Resistance of Osseous Element through Finite Element Modeling.
23. Chao, J., & López, V. (2007). *Failure analysis of a Ti6Al4V cementless HIP prosthesis. Engineering Failure Analysis, 14(5), 822–830.* doi:10.1016/j.engfailanal.2006.11.
24. Mughal, Uzair & Khawaja, Hassan & Moatamedi, M.. (2015). Finite element analysis of human femur bone. The International Journal of Multiphysics. 9. 101-108. 10.1260/1750-9548.9.2.101.
25. Filipovic, N. (2020). *The biomechanics of lower human extremities. Computational Modeling in Bioengineering and Bioinformatics, 179–210.* doi:10.1016/b978-0-12-819583-3.00006-0.
26. Mu Jung, J., & Sang Kim, C. (2014). Analysis of stress distribution around total hip stems custom-designed for the standardized Asian femur configuration. *Biotechnology, biotechnological equipment*, *28*(3), 525–532. https://doi.org/10.1080/13102818.2014.928450
27. Ghanem, M. Farag, M. Schneider, P. (2013). The short stem GHEs in total hip replacement – experience after 380 implantations. GMS Interdiscip Plast Reconstr Surg DGPW.
28. Hwang, S.(2014). Experience of Complications of Hip Arthroplasty. 10.5371/hp.2014.26.4.207
29. Bergmann, G. Bender, A. Dymke, J. Standardized Loads Acting in Hip Implants(2016). https://doi.org/10.1371/journal.pone.0155612
30. Fakhouri, S. Shimano, M. Araujo, C. (2014). Analysis of stress induced by screws in the vertebral fixation system. https://doi.org/10.1590/S1413-78522014000100002
31. Kutzner, I. Hallan, G. Hol, P. (2018) Early aseptic loosening of a mobile-bearing total knee replacement A case-control study with retrieval analyses. 10.1080/17453674.2017.1398012

32. Ridzwan, M. Shuib, S. Hassan, A.Y. (2007). Problem of Stress Shielding and Improvement to the Hip Implant Designs: A Review.
33. Wangen, H., Lereim, P., Holm, I., Gunderson, R., & Reikerås, O. (2008). Hip arthroplasty in patients younger than 30 years: excellent ten to 16-year follow-up results with a HA-coated stem. *International orthopaedics*, *32*(2), 203–208. https://doi.org/10.1007/s00264-006-0309-2.
34. Joshi, M. G., Advani, S. G., Miller, F., & Santare, M. H. (2000). Analysis of a femoral hip prosthesis designed to reduce stress shielding. Journal of Biomechanics, 33(12), 1655–1662. doi:10.1016/s0021-9290(00)00110-x.
35. Properties: E-Glass Fibre. (2020). Retrieved 22 September 2020, from https://www.azom.com/properties.aspx?ArticleID=764.
36. Elsner, Jonathan & Eliaz, Noam & Linder-Ganz, Eran. (2015). The Use of Polyurethanes in Joint Replacement. 10.1142/9781783267170_0009.